

Thermodynamic Properties of Natural Gas Mixtures Using Equations of State

Kh. Nasrifar* and O. Bolland

Department of Energy and Process Engineering

Norwegian University of Science and Technology (NTNU)

NO -7491 Trondheim, Norway

-
- Corresponding author
E-mail: khashayar.nasrifar@ntnu.no
Tel: +47 735 98462
Fax: +47 735 98390

Abstract

In this contribution, six cubic equations of state (EoS) are used to predict the thermo-physical properties of natural gas mixtures. One of the EoS is proposed in this work. This EoS is obtained by matching the critical fugacity coefficient of the EoS to the critical fugacity coefficient of methane. Special attention is given to the supercritical behavior of methane as it is the major component of natural gas mixtures and almost always supercritical at reservoir and surface conditions. Compared to the other EoS, the proposed EoS more accurately predicts the compressibility factors and speeds of sound data for natural gas mixtures. The average absolute error was found to be 0.47% for predicting the compressibility factors and 0.7% for the speeds of sound data. The obtained EoS was also used to predict thermal and equilibrium properties. In predicting the bubble point pressure of liquefied natural gas (LNG) mixtures, the EoS is quite successful and shows significant accuracy when compared to the other EoS. For predicting some other properties of natural gas mixtures, for instance, isobaric heat capacity, Joule-Thomson coefficient and dew points, the predictive capability of the EoS is comparable to the other EoS.

Keywords: Natural gas, thermodynamic property, equation of state.

Introduction

Predicting the thermodynamic properties of natural gas mixtures are important in gas industry-that is in production, processing, storage and transportation. Accurate values of natural gas compressibility factors and speeds of sound data are crucial in custody transfer operations. Other thermodynamic properties, e.g., saturated liquid density and bubble point pressure of liquefied natural gas (LNG) mixtures, are used in the design of liquefaction processes and storage facilities; Joule-Thomson coefficients are used in throttling processes and dew points are used in pipeline design.

There are accurate correlations/equations of state (EoS) for calculating natural gas properties. McCarty [1] reported an accurate extended corresponding states (ECS) model for LNG systems. Using ECS models, Estela-Urbe and Trusler [2] and Estela-Urbe et al. [3] predicted the compressibility factors, density, speeds of sound and bubble point pressures of natural gas mixtures quite accurately. Accurate models, for instance, AGA NX-19 [4] and MGERG-88 [5] are used in custody transfer for calculating compressibility factors of natural gas mixtures. The Benedict-Webb-Rubin [6] (BWR) EoS, modified Redlich and Kwong [7] EoS by Soave [8] (RKS) and Peng and Robinson [9] (PR) EoS are often used in the gas industry for predicting natural gas equilibrium properties.

Except the RKS and PR EoS, the other models are either complex or require many pure component constants and/or binary parameters [3]. For instance, the BWR EoS has 8 constants. The MGERG [5] model is not suitable for thermal properties calculations. The ECS models of Estela-Urbe and Trusler [2] and Estela-Urbe et al. [3] take the advantages of binary parameters, and therefore cannot be extended to natural gas mixtures with heavy fractions.

The RKS and PR EoS are often employed in the gas industry as predictive tools. When these two EoS are compared with the mentioned models above, they are rather accurate. Moreover, both EoS take the advantage of simplicity. They are reliable and predict the thermodynamic properties of natural gas mixtures with reasonable accuracy. In addition, these two EoS can be used for predicting the properties of natural gas mixtures containing heavy fractions.

Natural gas mixtures comprise supercritical methane as the major component. When the new findings in supercritical behavior of EoS are taken into account [10], an accurate EoS can be developed for application in the gas industry. The objective of this work is to obtain a predictive two-constant EoS. This EoS should exhibit an accurate description of thermodynamic properties of natural gas mixtures while preserving the outstanding characteristics of the RKS and PR equations.

Model Development

Natural gas mixtures comprises of many hydrocarbon and non-hydrocarbon constituents with methane as the major component. Heavy hydrocarbons up to C_{40} sometimes exist in natural gas mixtures. Nitrogen, carbon dioxide and hydrogen sulfide are usually the non-hydrocarbon components. While the gas phase properties of natural gas mixtures, to a large extent, result from the presence of methane, the equilibrium properties of the natural gas are affected by the presence of heavier hydrocarbons. An EoS that accurately describes the properties of methane and heavier hydrocarbons must therefore accurately predict the properties of natural gas mixtures.

The pressure and temperature of most natural gas mixtures, at reservoir and surface conditions, can be found up to 150 MPa and 500 K, respectively. At these conditions, nitrogen, methane and ethane are almost always supercritical while the

heaviest hydrocarbons are subcritical. In other words, to accurately describe the properties of natural gas mixtures, the supercritical behavior of methane and to a less extent nitrogen and ethane, and the subcritical behavior of heavy hydrocarbons should be accurately described. In an EoS, the subcritical and supercritical behavior of fluids not only attributes to the pressure-volume-temperature (*PVT*) relationship of the EoS but also to the temperature dependence of the α function. A general two constant EoS may be defined by [11]:

$$P = \frac{RT}{v-b} - \frac{a_c \alpha(T_r)}{(v + \delta_1 b)(v + \delta_2 b)} \quad (1)$$

with

$$b = \Omega_b \frac{RT_C}{P_C} \quad (2)$$

$$a_c = \Omega_a \frac{R^2 T_C^2}{P_C} \quad (3)$$

where P is the pressure, T is the temperature, v is the specific volume, R is the gas constant, b is the molar covolume, a is the attractive parameter, and Ω_b and Ω_a are two coefficients which depends on the constants δ_1 and δ_2 . The subscripts r and C stands for the reduced and critical properties. The second virial coefficient for eq 1 is expressed by:

$$\frac{B_{2,c} P_C}{RT_C} = \Omega_b - \Omega_a \quad (4)$$

where $B_{2,c}$ is the second virial coefficient at the critical point. Mathias [10] pointed out that the reduced second virial coefficient ($B_{2,c}P_c / RT_c$) of most fluids at the critical point is nearly -0.34. When this condition is applied to eq 4, one can obtain

$$\Omega_b - \Omega_a \approx -0.34 \quad (5)$$

Eq 5 would be the constraint for obtaining an EoS for natural gas mixtures.

Nasrifar and Bolland [12] improved Soave's α function on the basis of the equality of the second virial coefficient from the RKS EoS and square-well potential. The obtained α function, in general, improves the accuracy of the RKS EoS in predicting the pure component compressibility factor and the fugacity at supercritical temperatures. Accurate fugacity of pure compounds is particularly important, as shown by Flöter et al. [13], in calculating the fluid phase equilibria of asymmetric hydrocarbon mixtures containing methane. However, the fugacity of fluids for an EoS is usually fixed indirectly by correlating the EoS to the vapor pressure of pure compounds along the coexistence curve. It is also worth noting that all two-constant EoS similar in form to eq. 1 have a fixed value of fugacity at the critical point. For the RKS EoS, the critical fugacity coefficient is 0.6657 and 0.6457 for the PR EoS [11]. The reported value of the fugacity coefficient of methane [14] at the critical point is 0.6640, however. If eq 1 is to be used to predict the thermodynamic properties of methane (natural gas) in supercritical region, the starting point which is the critical point, should be predicted accurately. It should be noted that the accuracy of EoS in engineering is based on the adequacy of the critical point for predicting the subcritical and supercritical properties. As such, it is essential for an EoS of natural gas systems to predict the critical fugacity of methane (as the major component) accurately. On the

basis of this premise and eq 5 as the constraint, we concluded that $\delta_1 = \delta_2 = 1/\sqrt{3}$ would meet these requirements. Incorporating these values in eq 1, a new PVT relationship is obtained:

$$P = \frac{RT}{v-b} - \frac{a_c \alpha(T_r)}{(v+b/\sqrt{3})^2} \quad (6)$$

with

$$b = 0.079246 \frac{RT_c}{P_c} \quad (7)$$

$$a_c = 0.421875 \frac{R^2 T_c^2}{P_c} \quad (8)$$

The critical compressibility factor, second virial coefficient, and fugacity coefficient for eq 6 were found to be 0.329, -0.342, and 0.6640, respectively.

For the α function, the modified Soave's α function by Nasrifar and Bolland [12] is used:

$$\alpha(T_r) = \begin{cases} \left[1 + m(1 - \sqrt{T_r})\right]^2 & T_r \leq 1 \\ \frac{b_1}{T_r} + \frac{b_2}{T_r^2} + \frac{b_3}{T_r^3} & T_r > 1 \end{cases} \quad (9)$$

with

$$b_1 = 0.25(12 - 11m + m^2) \quad (10)$$

$$b_2 = 0.5(-6 + 9m - m^2) \quad (11)$$

$$b_3 = 0.25(4 - 7m + m^2) \quad (12)$$

where the parameter m was determined by correlating the vapor pressure of pure substances from the triple point to the critical point. These obtained parameters were correlated in terms of acentric factor (ω). The final correlation is expressed by:

$$m = 0.4857 + 1.6308\omega - 0.2089\omega^2 \quad (13)$$

where ω ranges from -0.216 to 0.8764.

Extension to Mixtures

The classical van der Waals mixing rules are used to extend eq 6 to mixtures:

$$b = \sum_j x_j b_j \quad (14)$$

$$a = \sum_i \sum_j x_i x_j a_{ij} \quad (15)$$

with

$$a_{ij} = \sqrt{a_i a_j} (1 - k_{ij}) \quad (16)$$

where x is the liquid/vapor mole fraction and k_{ij} is the binary interaction parameter. In

this work, $k_{ij} = 0$, otherwise it is stated.

Results and Discussion

Components in a natural gas mixture behave differently than in pure state. Nevertheless the accuracy of an EoS in predicting pure component properties significantly affects on the accuracy of the EoS in predicting natural gas properties. Table 1 presents the accuracy of eq 6 in predicting the vapor pressure of common

components in natural gas mixtures from the triple point to the critical point. Given in Table 1 are also predictions from the PR EoS, modified PR EoS by Gasem et al. [15] (PRGGPR), RKS EoS, modified Redlich and Kwong [7] by Twu et a. [16] (RKTCC), and modified RKS EoS by Nasrifar and Bolland [12] (RKSNB). With exception of the PR EoS, all other EoS predict the vapor pressure of pure substances with similar accuracy. The average absolute deviation defined by:

$$\%AAD = (100/n) \sum_j |cald_j - expl_j| / expl_j \quad (17)$$

is about 3% for these EoS and 8.14% for the PR EoS. Figure 1 shows a deviation plot for predicting the vapor pressure of some components in natural gas mixtures using eq 6. Clearly, deviations propagate around zero with reasonable accuracy except for H₂S and *i*-C₅H₁₂ at low reduced temperatures.

As mentioned before, the supercritical behavior of methane must be effective on the thermodynamic properties of natural gas mixtures. A property that can reflect the accuracy of eq 6 in predicting the supercritical behavior of methane is fugacity. Figure 2 displays the percent absolute deviation in predicting the fugacity of methane by use of eq 6. The temperature ranges from 195 K to 600 K and pressure from 1 MPa to 150 MPa. The deviations are larger at low temperatures and increases with pressure. However, up to 90 MPa, the deviations are remarkably small no matter what the temperature is. The %AAD was found to be 2.39% for eq 6. For the PR EoS, the %AAD was 8.5%, and 7.83%, 3.59%, 5.27% and 2.57% for the PRGGPR, RKS, RKTCC and RKSNB EoS, respectively. The RKSNB and eq 6 are remarkably superior compared to the others. This high accuracy attributes to the use of eq 9 as the α function for both EoS.

Table 2 gives the composition and code names for 20 LNG mixtures. The bubble point pressure and saturated liquid density of these LNG mixtures were predicted by eq 6 and compared with experimental data in Tables 3 and 4, respectively. Also given in Tables 3 and 4 are the predictions from the other EoS. Table 3 indicates that eq 6 predicts the bubble point pressure of LNG mixtures with significant accuracy, especially those mixtures devoid of nitrogen. A close look at Table 3 also indicates that the presence of even small amount of nitrogen causes the deviations to become large. The smallest %AAD for predicting the bubble point pressure of LNG mixtures containing nitrogen is 12.16%. This mixture contains 0.6% to 0.8% nitrogen and the predictions for mixtures with larger amount of nitrogen are worse. Nevertheless, the average %AAD for eq 6 is 10.1% which is better than the other EoS. The predictions might become better when binary interaction coefficients are introduced; however, in this work, we are only concerned with the predictive capability of the EoS. It is also worth considering that the RKS and RKS_{NB} predict the bubble point pressure, and as seen in Table 4, the saturated liquid density of LNG mixtures to the same accuracy. In fact, at conditions where these LNG mixtures were studied, methane is subcritical and nitrogen is slightly supercritical. In other words, the RKS_{NB} reduces to the RKS EoS and hence both have the same accuracy. The accuracy of the EoS in predicting the saturated liquid density of the LNG mixtures is shown in Table 4. Clearly, the RKS, RKS_{NB} and RKTCC predict the saturated liquid densities better than the other EoS with an average %AAD of 1.74%. The average %AAD for eq 6 is 4.66% and 10.76% and 10.95% for the PR and PRGGPR EoS, respectively. Table 4 also indicates that the accuracy of an EoS in predicting the liquid density of LNG mixtures is a consequence of the *PVT* relationship and nearly independent of the α function. Table 4 shows that the RKS, RKS_{NB}, RKTCC, PR and PRGGPR predict the liquid density

of LNG mixture with a similar ability. Further, Table 4 indicates that the accuracy of eq 6 lies between the RK family and PR family EoS in predicting the saturated liquid density of LNG mixtures.

Table 5 presents the compositions and code names for 14 natural gas mixtures used for predicting the compressibility factor and speeds of sound data. In Tables 6 and 7, the accuracy of the EoS is compared for predicting the compressibility factor and speeds of sounds data, respectively. Clearly, eq 6 is remarkably superior with respect to the other EoS for predicting these two properties. The average %AAD was found to be 0.47% for predicting the compressibility factors and 0.7% for the speeds of sound. When the RKS and RKS_{NB} are compared, it is seen that the use of eq 9 with the modified Soave's α function in RKS_{NB} improves the RKS EoS in predicting these two properties of natural gas mixtures.

Table 8 gives the compositions and code names for 9 other natural gas mixtures. These mixtures are used in calculating isobaric heat capacity, Joule-Thomson coefficient and vapor-liquid-equilibria (VLE) of natural gas mixtures. In Table 9, the accuracy of eq 6 in predicting the isobaric heat capacity of 4 natural gas mixtures is presented. With the exception of the RKTCC EoS, with an average %AAD of 2.3%, the other EoS predict the isobaric heat capacity of the natural gas mixtures with an average %AAD of about 1.4%. However, the RKS EoS with an %AAD of 1.34%, is slightly superior among the others. Eq 6 is ranked number 2 in this comparison.

Figure 3 shows Joule-Thomson coefficient for the natural gas mixture M16 as a function of pressure and temperature. As can be seen, the agreement with experimental data is quite good. The %AAD was found to be 5.03%. The same calculations were performed for the other EoS, and the %AAD was found to be

12.03%, 13.11%, 5.10%, 6.74% and 4.5%, respectively, for the PR EoS, PRGGPR, RKS, RKTCC, and RKS NB EoS.

Figure 4 depicts experimental and predicted bubble and dew points for a model system comprised of methane and *n*-eicosane at 323.15 K. Among the EoS used in this study, the RKTCC EoS predicts the experimental values more accurately than the others while the PR EoS predicts with the worst accuracy. The other EoS including eq 6 lie between these two extremes. For clarity, only the predictions from eq 6 are illustrated. Nevertheless, because of large non ideality for these asymmetric mixtures, none of the EoS is predictive enough to agree with the experimental data. However, the *VLE* of binary asymmetric mixtures can easily be correlated, as shown in Figure 5, for the same system at 353.15 K.

The accurate prediction of equilibrium ratios for components in a gas mixture is of primary concern in *VLE* calculations. Figure 6 shows equilibrium ratios of the natural gas mixture M19 as a function pressure at 366.44 K. As can be seen, the agreement between the predictions by eq 6 and experimental data is quite good except for nitrogen and carbon dioxide. Unless the compositions of these components are large, this inaccuracy will not pose problem. However, the inaccuracy might be alleviated by use of k_{ij} in eq 16.

In Table 10, experimental and predicted dew point pressures and liquid compositions for the gas condensate mixture M20 are compared. In order to perform calculations, the C_{7+} fraction was split into 12 single carbon number groups (SNG) using the logarithm distribution described by Pedersen et al. [35]. The critical properties and acentric factor of each group were determined by Twu's correlations [36]. After characterizing the C_{7+} fraction, the *VLE* calculations were performed. The results are given in Table 10. Comparison with experimental data indicates that PR

EoS accurately predicts the natural gas mixture dew point at 367 K. The RKS NB, PRGGPR and eq 6 are next best in agreement with the experimental data while the RKTCC is the worst among the others. Nevertheless, none of the EoS accurately predicts the liquid phase compositions, especially for methane and the heavy fraction.

Table 11 gives flash yields for gas condensate mixture M21. The heavy fraction was characterized similarly to the gas condensate mixture M20. Although the predictions are similar in accuracy, the PR and PRGGPR are slightly more accurate.

Figure 7 shows phase envelope for the natural gas mixture M22. In addition to eq 6, the RKTCC, RKS NB and PRGGPR were used to predict the phase envelope. The phase envelope predicted by the PRGGPR is clearly the least accurate among the others while eq 6, RKTCC and RKS NB are similar in accuracy. Figure 8 shows the phase envelope for natural gas mixture M23. The experimental values are from Avila et al. [33] and predicted values from eq 6, and three other EoS: Schmidt and Wenzel [37] (SW), modified Patel and Teja [38] by Valderrama [39] (PTV) and Guo and Du [40] (GD). The SW EoS and eq 6 are clearly in better agreement with experimental data when compared to the other EoS. While eq 6 slightly underestimates the experimental data, the SW EoS overestimates. The PTV and GD EoS predictions lie inside the experimental phase envelope.

Conclusions

A two-constant cubic EoS is introduced by matching the critical fugacity coefficient of the EoS equal to the fugacity coefficient of methane at the critical point. A recently augmented Soave's α function has been used for the temperature dependence of the attractive parameter in the EoS. The developed EoS has predicted the natural gas compressibility factors and speeds of sound data with significant

accuracy. The EoS has also accurately predicted the bubble point pressures of LNG mixtures. In predicting these properties, the new EoS has shown remarkable superiority when compared to other two-constant EoS. The accuracy of the EoS in predicting other natural gas properties, i.e., isobaric heat capacity, Joule-Thomson coefficient, and calculating dew points, phase envelopes and flash yields is similar to the other EoS.

Acknowledgement

The authors express their appreciations to Statoil, Norway, for supporting this work.

Literature cited

- [1] R. D. McCarty, *J. Chem. Thermodyn.* 14 (1982) 837-854.
- [2] J. F. Estela-Uribe, J. P. E. Trusler, *Fluid Phase Equilib.* 183-184 (2001) 21-29.
- [3] J. F. Estela-Uribe, A. De Mondoza, J. P. E. Trusler, *Fluid Phase Equilib.* 216 (2004) 59-84.
- [4] AGA Report No. 3 = ANSI/API 2530. *Orifice Metering of Natural Gas*; American National Standard Institute (ANSI): New York, 1978.
- [5] M. Jaeschke, S. Audibert, P. van Caneghem, A. E. Humphreys, R. Janssen-van Rosmalen, Q. Pellei, J. P. Michels, J. A. Schouten, C. A. ten Seldam, *High Accuracy Compressibility Factor for Natural Gases and Similar Mixtures by Use of a Truncated Virial Equation*. GERG Technical Monograph TM2, 1989.
- [6] M. Benedict, G. B. Webb, L. C. Rubin, *J. Chem. Phys.* 8 (1940) 334-345.
- [7] O. Redlich, J. N. S. Kwong, *Chem. Rev.* 44 (1949) 233-244.
- [8] G. Soave, *Chem. Eng. Sci.* 27 (1972) 1197-1203.

- [9] D.-Y. Peng, D. B. Robinson, *Ind. Eng. Chem. Fundam.* 15 (1976) 59-64.
- [10] P. M. Mathias, *Ind. Eng. Chem. Res.* 42 (2003) 7037-7044.
- [11] M. L. Michelsen, J. M. Mollerup, *Thermodynamic Models, Fundamentals and Computational Aspects*. Tie-Line Publication: Holte, Denmark, 2004.
- [12] Kh. Nasrifar, O. Bolland, *Ind. Eng. Chem. Res.* 43 (2004) 6901-6909.
- [13] E. Flöter, Th. W. de Loos, J. de Swaan Arons, *Ind. Eng. Chem. Res.* 37 (1998) 1651-1662.
- [14] B. A. Younglove, J. F. Ely, *J. Phys. Chem. Ref. Data.* 16 (1987) 577-798.
- [15] K. A. M. Gasem, W. Gao, Z. Pan, R. L. Robinson, Jr. *Fluid Phase Equilib.* 181 (2001) 113-125.
- [16] C. H. Twu, J. E. Coon., J. R. Cunningham, *Fluid Phase Equilib.* 105 (1995) 61-69.
- [17] T. E. Daubert, R. P. Danner, *Physical and Thermodynamic Properties of Pure Chemicals, Data Compilation*; Hemisphere Publishing Corp.: London, U.K., 1992.
- [18] W. Wagner, K. M. de Reuck, (IUPAC). *Methane. International Thermodynamic Tables of the Fluid State*; Blackwell: Oxford, U. K., Vol. 13, 1996.
- [19] W. M. Haynes, M. J. Hiza, *J. Chem. Thermodyn.* 9 (1977) 179-187.
- [20] M. J. Hiza, W. M. Haynes, *J. Chem. Thermodyn.* 12 (1980) 1-10.
- [21] W. M. Haynes, *J. Chem. Thermodyn.* 14 (1982) 603-612.
- [22] J. M. Magee, W. M. Haynes, M. J. Hiza, *J. Chem. Thermodyn.* 29 (1997) 1439-1454.
- [23] C.-A. Hwang, P. P. Simon, H. Hou, K. R. Hall, J. C. Holste, K. N. Marsh, *J. Chem. Thermodyn.* 29 (1997) 1455-1472.

- [24] L. Čapla, P. Buryan, J. Jedelský, M. Rottner, J. Linek, *J. Chem. Thermodyn.* 34 (2002) 657-667.
- [25] M. F. Costa Gomes, J. P. M. Trusler, *J. Chem. Thermodyn.* 30 (1998) 1121-1129.
- [26] B. A. Younglove, N. V. Frederick, R. D. McCarty, *Speed of Sound Data and Related Models for Mixtures of Natural Gas Constituents*. NIST Monograph 178, 1993.
- [27] G. Ernst, R. Keil, H. Wirbser, M. Jaeschke, *J. Chem. Thermodyn.* 33 (2001) 601-613.
- [28] A. Barreau, P. Janneteau, K. Gaillard, *Fluid Phase Equilib.* 119 (1996) 197-212.
- [29] L. Yarborough, J. L. Vogel, *Chem. Eng. Symp. Ser.* 63 (1967) 63, 1-9.
- [30] A. E. Hoffmann, J. S. Crump, C. R. Hocott, *Petroleum Trans. AIME* 198 (1953) 1-10.
- [31] A. Firoozabadi, Y. Hekim, D. L. Katz, *Can. J. Chem. Eng.* 56 (1978) 610-615.
- [32] S. Avila, S. T. Blanco, I. Velasco, E. Rauzy, S. Otín, *Energy & Fuels* 16 (2002) 928-934.
- [33] S. Avila, S. T. Blanco, I. Velasco, E. Rauzy, S. Otín, *Ind. Eng. Chem. Res.* 41 (2002) 3714-3721.
- [34] H. J. van der Kooi, E. Flöter, Th. W. de Loos, *J. Chem. Thermodyn.* 27 (1995) 847-861.
- [35] K. S. Pedersen, A. L. Blilie, K. K. Meisingset, *Ind. Eng. Chem. Res.* 31 (1992) 1378-1384.
- [36] C. H. Twu, *Fluid Phase Equilib.* 16 (1984) 137-150.
- [37] G. Schmidt, H. Wenzel, *Chem. Eng. Sci.* 35 (1980) 1503-1512.
- [38] N. C. Patel, A. S. Teja, *Chem. Eng. Sci.* 37 (1982) 463-473.

- [39] J. O. Valderrama, *J. Chem. Eng. Jpn.* 23 (1990) 87-91.
- [40] T.-M. Guo, L. Du, *Fluid phase Equilib.* 52 (1989) 47-57.

Table 1

Accuracy (%AAD) of the EoS in predicting the vapor pressure of some natural gas components (experimental data from Daubert and Danner [17])

Component	T_r range	This work	RKS/ RKSNB	RKTCC	PR	PRGGPR
H ₂ S	0.50-1	3.04	2.3	3.75	3.91	3.42
CO ₂	0.71-1	0.99	0.44	0.11	0.52	0.14
C ₁	0.48-1	1.66	2.02	0.26	0.5	1.06
C ₂	0.30-1	2.28	3.6	1.83	3.46	1.45
C ₃	0.23-1	2.33	3.08	7.37	9.37	3.53
<i>i</i> -C ₄	0.29-1	8.55	7.17	4.4	16.33	9.09
<i>n</i> -C ₄	0.32-1	1.8	2.3	3	4.33	0.85
<i>i</i> -C ₅	0.25-1	2.33	2.5	7.78	11.81	1.25
<i>n</i> -C ₅	0.30-1	6.76	6.04	2.35	14.79	8.39
<i>n</i> -C ₆	0.35-1	4.8	4.88	2.32	8.44	5.03
<i>n</i> -C ₈	0.38-1	2.51	2.11	3.5	3.53	1.79
<i>n</i> -C ₁₂	0.40-1	2.08	1.69	2.34	9.00	3.65
<i>n</i> -C ₁₆	0.40-1	4.36	3.54	4	11.73	2.18
<i>n</i> -C ₂₀	0.40-1	3.26	4.03	4.35	25.9	7.04
C ₆ H ₆	0.49-1	1.63	0.78	1.11	1.59	1.67
<i>cyc</i> -C ₅	0.35-1	1.79	1.15	0.87	5.10	2.67
Average		3.14	2.98	3.08	8.14	3.33

Table 2

LNG mixtures compositions and code names (experimental data from Haynes and Hiza [19], Hiza and Haynes [20] and Haynes [21])

Code	N ₂	C ₁	C ₂	C ₃	<i>i</i> -C ₄	<i>n</i> -C ₄	<i>i</i> -C ₅	<i>n</i> -C ₅
LNG1		0.8604,	0.0460,	0.0479,	0.0457,			
		0.85378	0.05178	0.0470	0.04741			
LNG2	0.04801	0.8094	0.04542	0.0505	0.04667			
LNG3		0.8534,	0.07895,	0.04729,	0.00854,	0.00992,	0.00097,	0.00089,
		0.75442	0.15401	0.06950	0.00978	0.00978	0.00089	0.00083
LNG4	0.0484	0.8526	0.0483	0.0507				
LNG5		0.84558-	0.05042-	0.4038-	0.0053-	0.00705-		
		0.85892	0.11532	0.01341	0.02577	0.02901		
LNG6	0.049	0.8060	0.0468	0.0482	0.050			
LNG7	0.0554	0.7909	0.056	0.0500		0.0477		
LNG8	0.00601-	0.8130-	0.0475-	0.02154-	0.00300-	0.00306-		
	0.0425	0.90613	0.08477	0.0298	0.0241	0.0242		
LNG9		0.85133,	0.05759,	0.04808,		0.02450,		
		0.84566	0.07924	0.05060		0.04300		
LNG10	0.00599-	0.74275-	0.06537-	0.02200-	0.00291-	0.00284-	0.00010-	0.00011-
	0.00859	0.90068	0.16505	0.06742	0.01336	0.01326	0.00223	0.00216
LNG11		0.85341	0.07898	0.04729	0.00854	0.00992	0.00097	0.00089
LNG12		0.86040	0.04600	0.04790	0.0457			
LNG13	0.0484	0.8094	0.04542	0.05050	0.04628			
LNG14	0.0484	0.8526	0.0453	0.0537				
LNG15		0.85443	0.05042	0.04038	0.02577	0.02900		
LNG16	0.049	0.8060	0.0468	0.0482	0.0500			
LNG17	0.0554	0.7909	0.056	0.05		0.0477		
LNG18	0.0425	0.8130	0.0475	0.0487	0.0241	0.0242		
LNG19		0.85133	0.05759	0.04808		0.0430		
LNG20	0.00599	0.74275	0.16505	0.06547	0.00843	0.00893	0.00069	0.00269

Table 3

Accuracy (%AAD) of the EoS in predicting bubble point pressure of the LNG mixtures

Code	T range (K)	n	This work	RKS/ RKS NB	RKTCC	PR	PRGGPR
LNG1	115-135	9	0.95	3.04	1.63	1.67	2.71
LNG2	115-130	4	14.74	16	15.4	17.75	17.75
LNG3	110-130	9	1.6	4.01	1.80	2.06	3.35
LNG4	105-120	4	16.9	18.32	17.82	19.44	19.75
LNG5	105-130	12	1.71	4.21	2.04	2.15	3.51
LNG6	105-120	4	25.44	26.72	26.02	28.32	28.25
LNG7	105-130	6	15.88	17.38	16.58	18.7	18.78
LNG8	115-130	9	0.75	2.81	1.39	1.47	2.50
LNG9	105-130	15	14.76	16.56	15.54	16.42	17.06
LNG10	110-130	13	12.16	14.18	12.85	13.76	14.49
LNG11	110-130	5	1.08	3.20	1.19	1.25	2.57
LNG12	115-135	5	0.81	2.63	1.37	1.37	2.38
LNG13	115-130	4	14.75	16	15.39	17.75	17.75
LNG14	105-120	4	16.9	18.32	17.82	19.44	19.75
LNG15	105-120	4	3.31	6.31	2.82	3.29	5.04
LNG16	105-120	4	25.44	26.72	26.02	28.32	28.25
LNG17	105-110	2	24.53	25.88	25.05	27.91	27.58
LNG18	105-120	4	32.7	33.93	33.14	35.2	35.18
LNG19	115-135	5	0.83	2.71	1.41	1.50	2.47
LNG20	110-125	4	21.15	23.12	21.57	22.6	23.28
Overall		126	10.1	12	10.65	11.55	12.29

Table 4

Accuracy (%AAD) of the EoS in predicting saturated liquid density of the LNG mixtures

Code	<i>T</i> range (K)	n	This work	RKS/ RKSNB	RKTCC	PR	PRGGPR
LNG1	115-135	9	4.3	1.98	1.96	10.55	10.74
LNG2	115-130	4	4.59	1.7	1.68	10.86	11.06
LNG3	110-130	9	4.61	1.89	1.9	10.56	10.75
LNG4	105-120	4	5.58	0.84	0.91	11.8	11.97
LNG5	105-130	12	4.63	1.75	1.77	10.76	10.94
LNG6	105-120	4	4.99	1.64	1.62	10.78	10.99
LNG7	105-130	6	4.82	1.67	1.65	10.82	11.02
LNG8	115-130	9	4.34	1.95	1.93	10.58	10.77
LNG9	105-130	15	4.8	1.45	1.48	11.17	11.34
LNG10	110-130	13	4.54	1.9	1.91	10.58	10.76
LNG11	110-130	5	4.69	1.67	1.69	10.81	11.05
LNG12	115-135	5	4.23	1.99	1.98	10.55	10.74
LNG13	115-130	4	4.59	1.7	1.68	10.86	11.06
LNG14	105-120	4	5.58	0.84	0.91	11.8	11.97
LNG15	105-120	4	4.61	2.05	2.02	10.3	10.51
LNG16	105-120	4	4.99	1.64	1.62	10.78	10.99
LNG17	105-110	2	5.17	1.65	1.61	10.69	10.92
LNG18	105-120	4	4.91	1.73	1.69	10.68	10.9
LNG19	115-135	5	4.2	2.06	2.02	10.46	10.65
LNG20	110-125	4	4.33	2.33	2.33	9.99	10.18
Overall		126	4.66	1.74	1.74	10.76	10.95

Table 5

Natural gas mixtures compositions and code names for calculating compressibility factors and speeds of sound data

Component	M1 _[22,23]	M2 _[22,23]	M3 _[22,23]	M4 _[22,23]	M5 _[22,23]	M6 _[24]	M7 _[24]	M8 _[24]	M9 _[25]	M10 _[25]	M11 _[26]	M12 _[26]	M13 _[26]	M14 _[26]
He							0.00015							
O ₂							0.00011							
N ₂	0.00269	0.03134	0.13575	0.05703	0.01007	0.00841	0.01474	0.05751		0.09922	0.00262	0.03113	0.00718	0.00537
CO ₂	0.00589	0.00466	0.00994	0.07592	0.01498	0.00066	0.00647	0.00052		0.02000	0.00597	0.00500	0.00756	0.01028
C ₁	0.96580	0.90644	0.81299	0.81203	0.85898	0.98352	0.90362	0.92436	0.84902	0.80051	0.96561	0.90708	0.83980	0.74348
C ₂	0.01815	0.04553	0.03294	0.04306	0.08499	0.00511	0.05708	0.01285	0.15098	0.05023	0.01829	0.04491	0.13475	0.12005
C ₃	0.00405	0.00833	0.00637	0.00894	0.02296	0.00153	0.01124	0.00348		0.03004	0.00410	0.00815	0.00943	0.08251
<i>i</i> -C ₄	0.00099	0.00100	0.00101	0.00148	0.00351	0.00021	0.00301	0.00041			0.00098	0.00106	0.00040	
<i>n</i> -C ₄	0.00102	0.00156	0.00100	0.00155	0.00347	0.00031	0.00169	0.00046			0.00098	0.00141	0.00067	0.03026
<i>i</i> -C ₅	0.00047	0.00030			0.00051	0.00008	0.00059	0.00015			0.00046	0.00027	0.00013	
<i>n</i> -C ₅	0.00032	0.00045			0.00053	0.00011	0.00029	0.00014			0.00032	0.00065	0.00008	0.00575
<i>n</i> -C ₆	0.00063	0.00040				0.00005	0.00058	0.00012			0.00067	0.00034		0.00230
<i>n</i> -C ₇						0.00001	0.00035							
<i>n</i> -C ₈						0.000003	0.00008							

Table 6

Accuracy (%AAD) of the EoS in predicting compressibility factor for natural gas mixtures

Code	n	T range (K)	P range (MPa)	This work	RKSNB	RKS	RKTCC	PR	PRGGPR
M1	143	225-350	0.19-34.27	0.52	1.25	1.37	2.15	1.68	1.53
M2	144	225-350	0.20-34.50	0.44	1.16	1.31	2.07	1.76	1.6
M3	144	225-350	0.18-34.65	0.3	0.84	1.07	1.67	1.86	1.7
M4	168	225-350	0.19-33.13	0.47	0.71	0.82	1.36	2.48	2.32
M5	125	250-350	0.19-32.95	0.53	1.31	1.46	2.32	1.97	1.81
M6	28	253-323	0.99-15.00	0.7	1.5	1.67	2.72	1.89	1.7
M7	28	253-323	1.00-15.02	0.66	1.53	1.72	2.87	2.09	2.6
M8	28	253-323	1.00-15.00	0.54	1.32	1.56	2.52	1.96	1.76
Overall	808			0.47	1.08	1.23	1.97	1.97	1.83

Table 7

Accuracy (%AAD) of the EoS in predicting speeds of sound for natural gas mixtures

Code	n	T Range (K)	P Range (MPa)	This work	RKSNB	RKS	RKTCC	PR	PRGGPR
M9	36	250-350	0.50-20	1.69	1.71	2.12	2.29	2.24	1.98
M10	35	250-350	0.50-20	1.04	1.11	1.77	1.7	1.66	1.34
M11	83	250-350	0.50-10.71	0.46	0.9	1.31	1.62	1.03	0.83
M12	82	250-350	0.65-10.88	0.47	0.74	1.11	1.32	1.09	0.87
M13	91	250-350	0.50-10.40	0.68	1.19	1.54	1.7	1.11	0.98
M14	44	300-350	0.42-10.40	0.56	1.25	1.77	1.96	1	0.82
Overall	371			0.7	1.08	1.5	1.69	1.24	1.03

Table 8

Natural gas mixtures compositions and code names for calculating isobaric heat capacity, Joule-Thomson coefficient and *VLE*

Component	M15 ^[27]	M16 ^[27]	M17 ^[28]	M18 ^[28]	M19 ^[29]	M20 ^[30]	M21 ^[31]	M22 ^[32]	M23 ^[33]
N ₂		0.09939	0.03187	0.00496	0.0048		0.0008	0.0048	0.05651
CO ₂		0.02090	0.01490		0.0015		0.0244		0.00284
C ₁	0.84874	0.79942	0.88405	0.89569	0.8064	0.9135	0.8210	0.887634	0.833482
C ₂	0.15126	0.05029	0.05166	0.08348	0.0593	0.0403	0.0578	0.0854	0.07526
C ₃		0.03000	0.01176	0.01197	0.0298	0.0153	0.0287	0.0168	0.02009
<i>i</i> -C ₄			0.00149	0.00149			0.0056	0.0022	0.00305
<i>n</i> -C ₄			0.00226	0.00226		0.0082	0.0123	0.0029	0.0052
<i>i</i> -C ₅			0.00056	0.00015			0.0052	0.000182	0.0012
<i>n</i> -C ₅			0.00049		0.0430	0.0034	0.0060	0.000084	0.00144
<i>i</i> -C ₆			0.000216						
<i>n</i> -C ₆			0.000136			0.0039	0.0072		0.00068
C ₆ H ₆			0.000272						
<i>cyc</i> -C ₆			0.000065						
<i>i</i> -C ₇			0.00010						
<i>n</i> -C ₇			0.000041		0.0308				0.000138
CH ₃ - <i>cyc</i> -C ₆			0.000052						
C ₆ H ₅ CH ₃			0.000030						
<i>i</i> -C ₈			0.000029						
<i>n</i> -C ₈			0.000008						0.00011
<i>i</i> -C ₉			0.000009						
<i>n</i> -C ₉			0.000002						
<i>n</i> -C ₁₀					0.0244				
C ₇₊						1.54 ^a	3.10 ^b		

^a C₇₊ specification: SG (60/60)=0.7961, MW=138.78, ^b C₇₊ specification: SG (60/60)=0.7740, MW=132

Table 9

Accuracy (%AAD) of the EoS in predicting isobaric heat capacity of natural gas mixtures

Code	n	T range (K)	P range (MPa)	This work	RKSNB	RKS	RKTCC	PR	PRGGPR
M15	56	250-350	0.6-30	1.5	1.61	1.49	2.2	1.9	1.9
M16	54	250-350	0.6-30	0.95	1.02	0.98	1.41	1.55	1.54
M17	30	308-406	15-40	1.13	1.16	0.96	2.52	0.8	0.73
M18	30	308-406	15-40	2.3	2.34	2.07	3.87	0.99	1.04
Overall	170			1.4	1.47	1.34	2.3	1.43	1.43

Table 10

Experimental [30] and predicted dew points for the gas condensate mixture M20

Component	Vapor (mol%)	Liquid (mol%)						
		Experimental	This work	RKSNB	RKS	RKTCC	PR	PRGGPR
C ₁	91.35	52.00	63.326	62.798	62.510	62.010	60.153	60.104
C ₂	4.03	3.81	4.454	4.454	4.485	4.521	4.401	4.420
C ₃	1.53	2.37	2.315	2.326	2.346	2.380	2.347	2.3440
<i>n</i> -C ₄	0.82	1.72	1.698	1.711	1.726	1.756	1.758	1.7420
<i>n</i> -C ₅	0.34	1.20	0.936	0.946	0.954	0.969	0.987	0.9720
<i>n</i> -C ₆	0.39	2.06	1.409	1.420	1.439	1.456	1.510	1.4760
C ₇₊	1.54	36.84	25.862	26.345	26.54	26.908	28.844	28.942
Dew point Pressure (MPa)		26.46	28.806	28.867	29.63	31.251	26.808	28.13

Table 11

Experimental [31] and predicted flash yields for the retrograde condensation of mixture M21

T(K)	P(MPa)	L/F ^a						
		Experimental	This work	RKSNB	RKS	RKTCC	PR	PRGGPR
278.15	14.6	0.1106	0.1727	0.1712	0.1703	0.1608	0.1694	0.1649
278.15	20.8	0.0993	0.1077	0.1122	0.1152	0.1276	0.0915	0.1025
318.15	14.6	0.0659	0.1010	0.0997	0.0988	0.0956	0.0946	0.0931
318.15	20.8	0.0333	0.0857	0.0853	0.0862	0.0877	0.0746	0.0754

^a L/F is the liquid to feed molar ratio

Figure Captions

Figure 1. Percent bias between experimental [17] and predicted vapor pressure of some natural gas constituents from the triple point to the critical point. The predictions are from eq 6 and %bias is defined by $\%bias = (100)(cald - expl)/expl$.

Figure 2. Percent absolute deviations between the IUPAC-recommended [18] and predicted fugacity of methane as functions of temperature and pressure. The predictions are from eq 6 and %Dev is defined by $\%Dev = (100)|cald - expl|/expl$.

Figure 3. Experimental [27] and predicted Joule-Thomson coefficients for the natural gas mixture M16.

Figure 4. Experimental [34] and predicted phase equilibria for the natural gas model mixture $CH_4 + n-C_{20}H_{42}$ at 323.15 K.

Figure 5. Experimental [34], predicted and correlated phase equilibria for the natural gas model mixture $CH_4 + n-C_{20}H_{42}$ at 353.15 K.

Figure 6. Experimental [29] and predicted equilibrium ratios for the natural gas mixture M19.

Figure 7. Experimental [32] and predicted phase envelopes for the natural gas mixture M22

Figure 8. Experimental [33] and predicted phase envelopes for the natural gas mixture M23

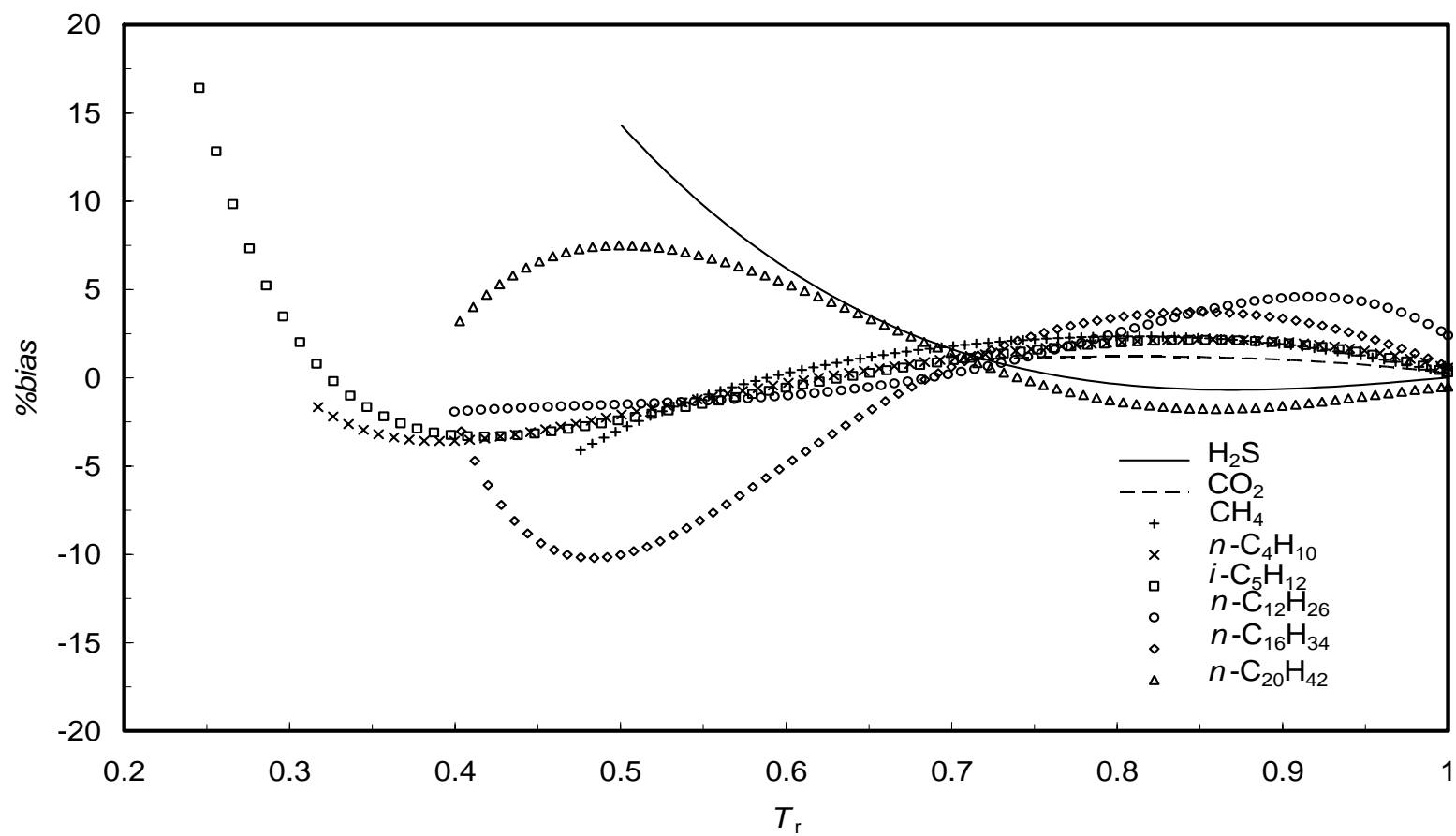


Figure 1.

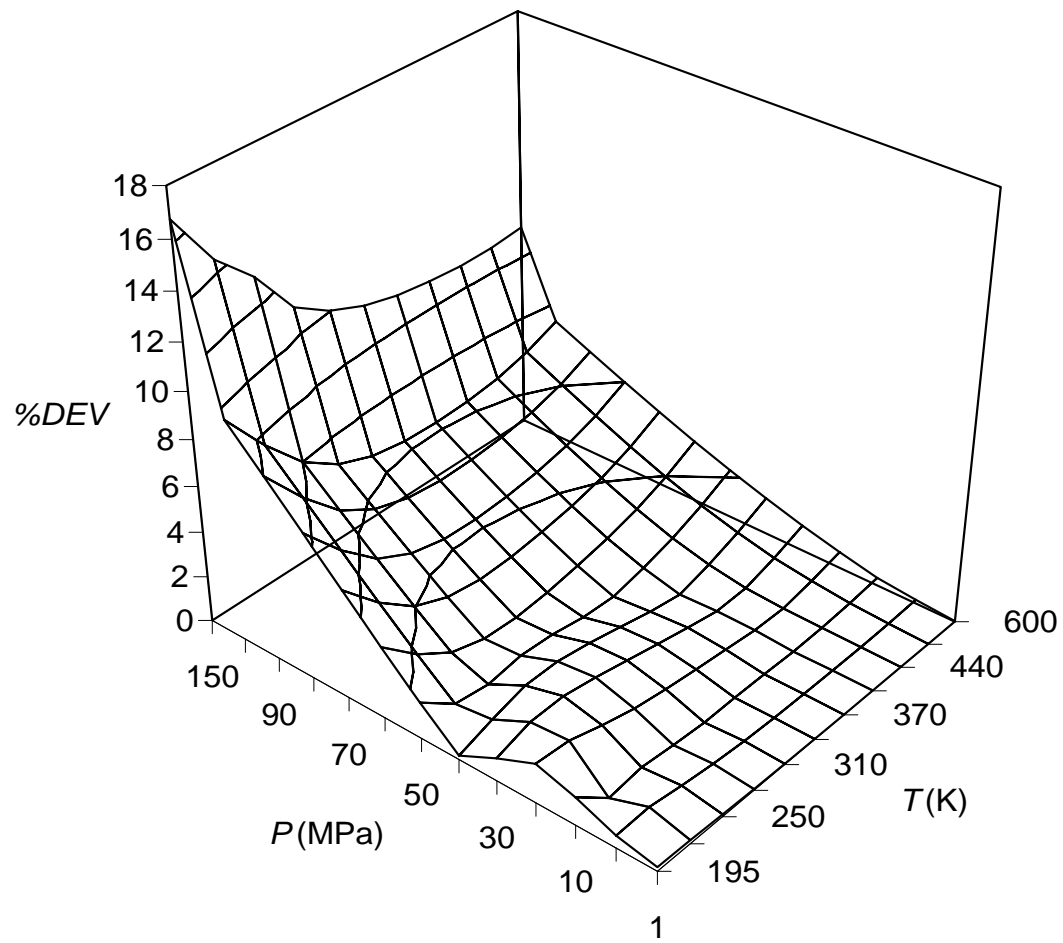


Figure 2.

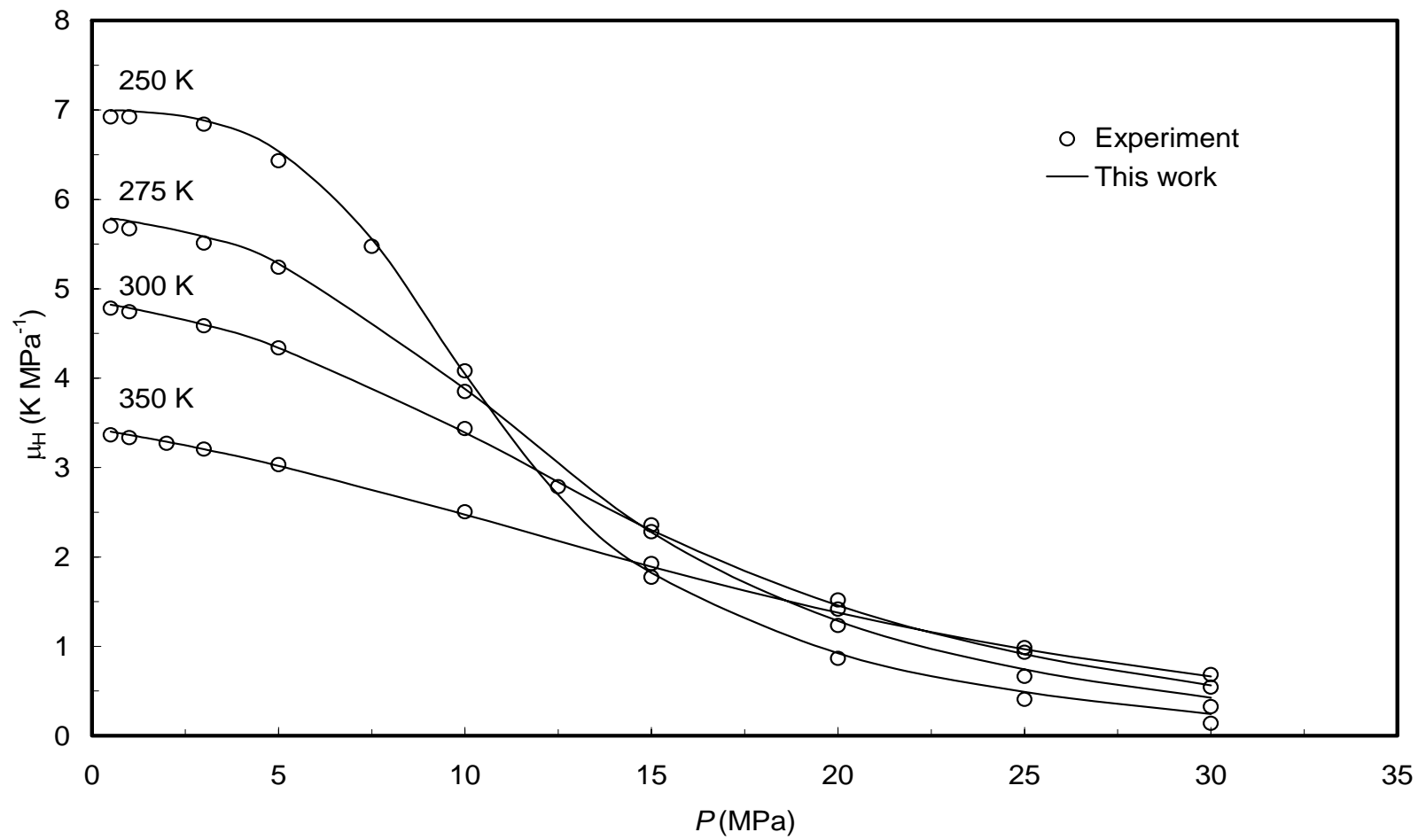


Figure 3.

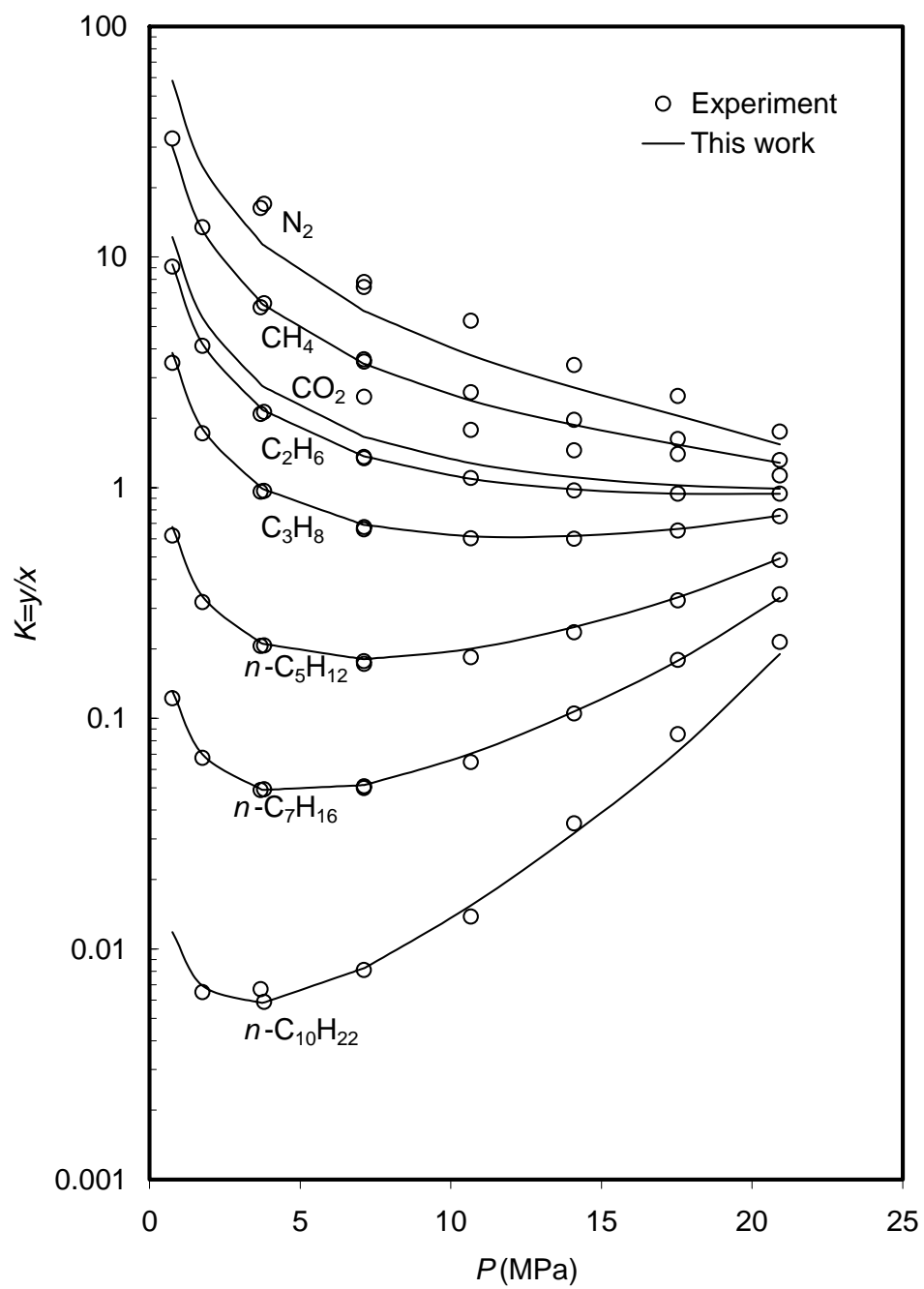


Figure 4.

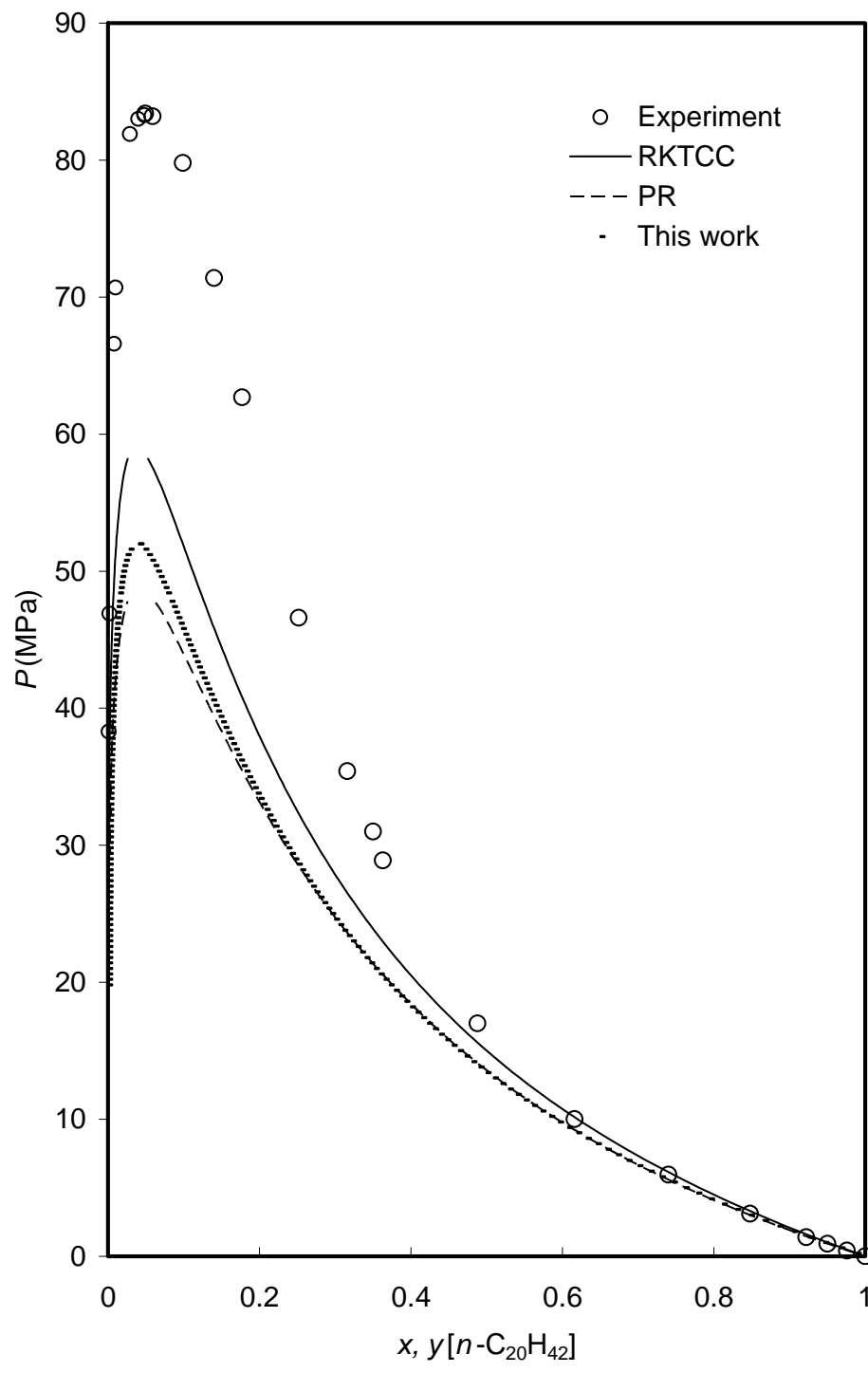


Figure 5.

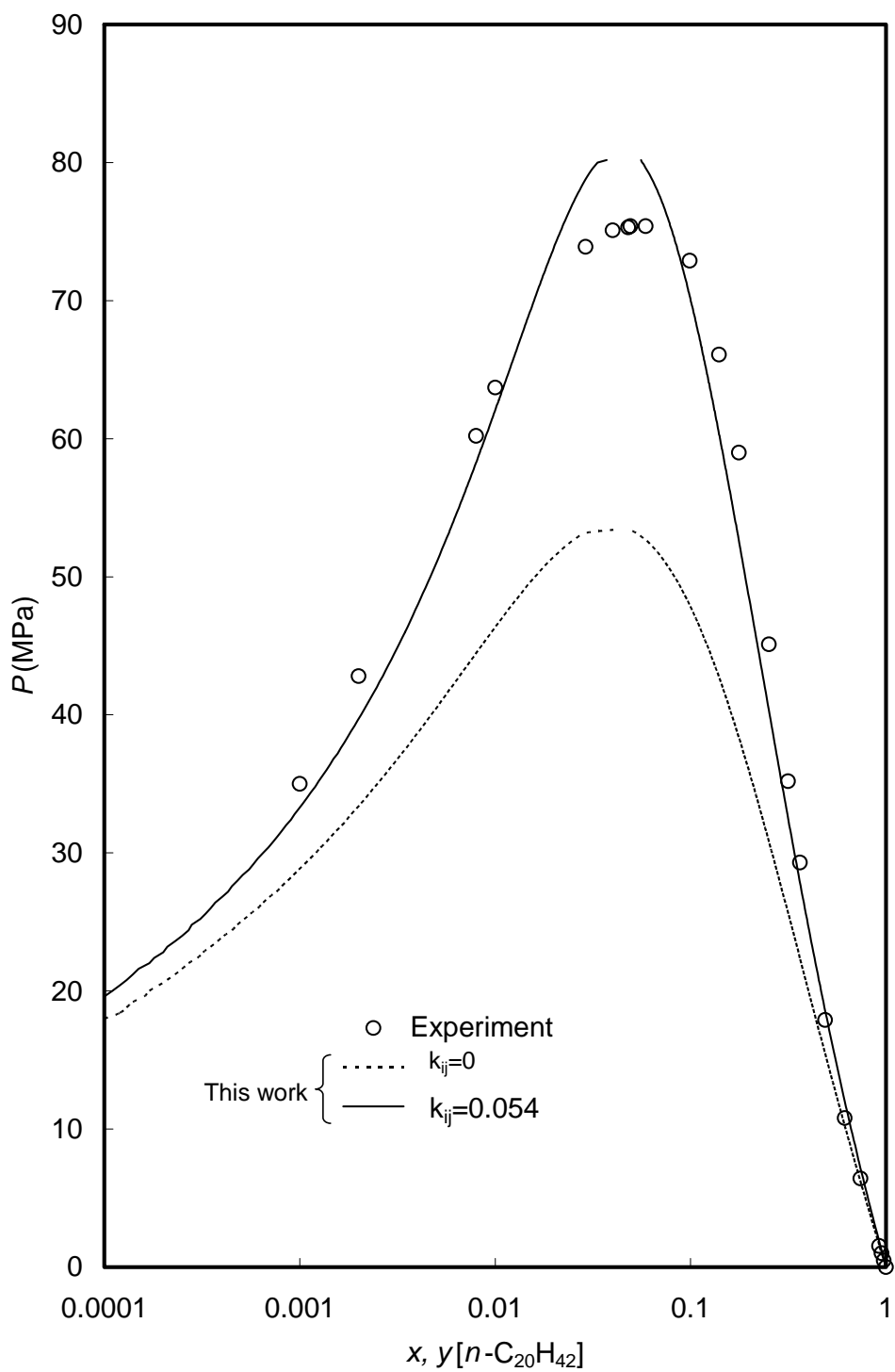


Figure 6.

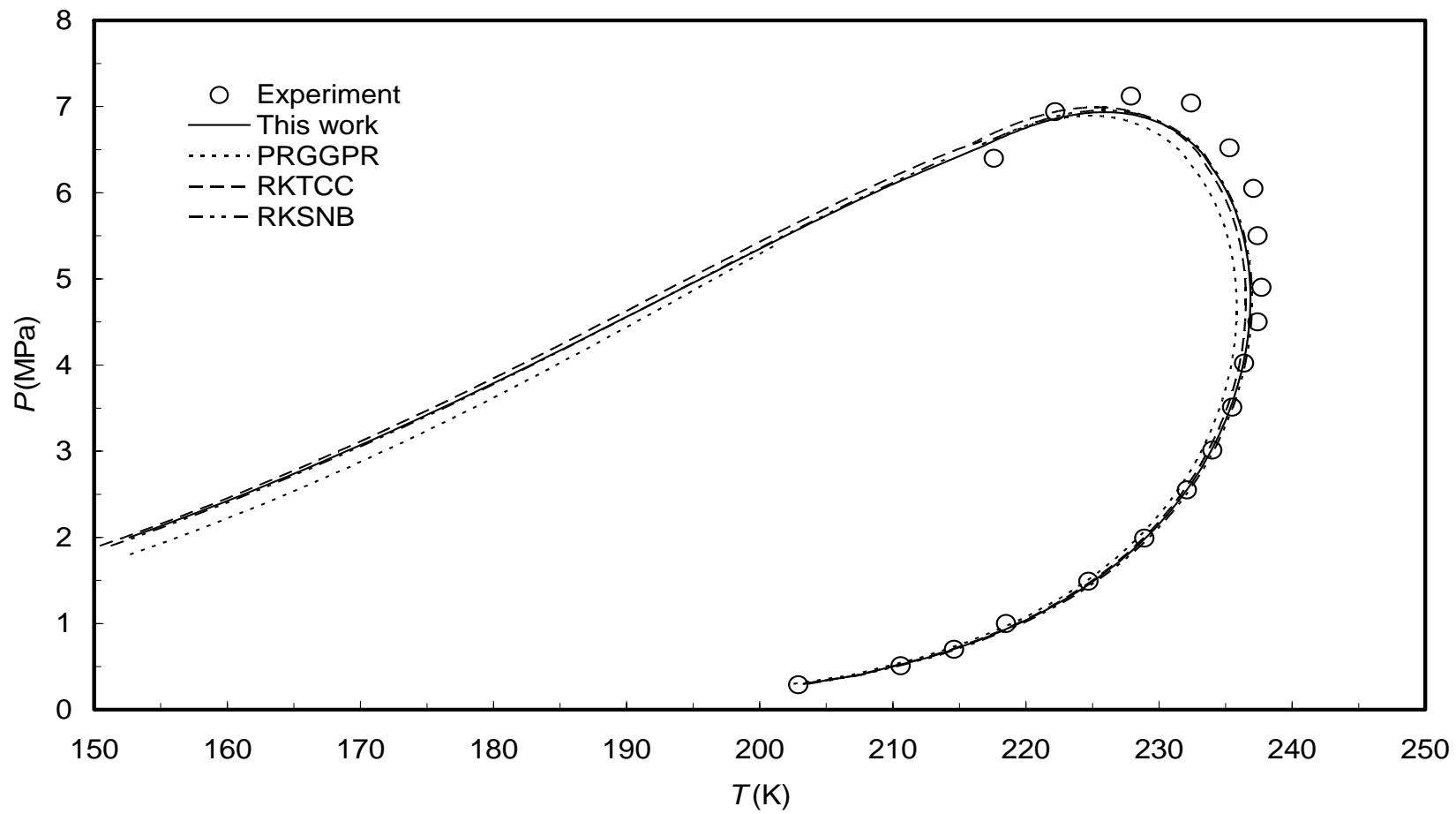


Figure 7.

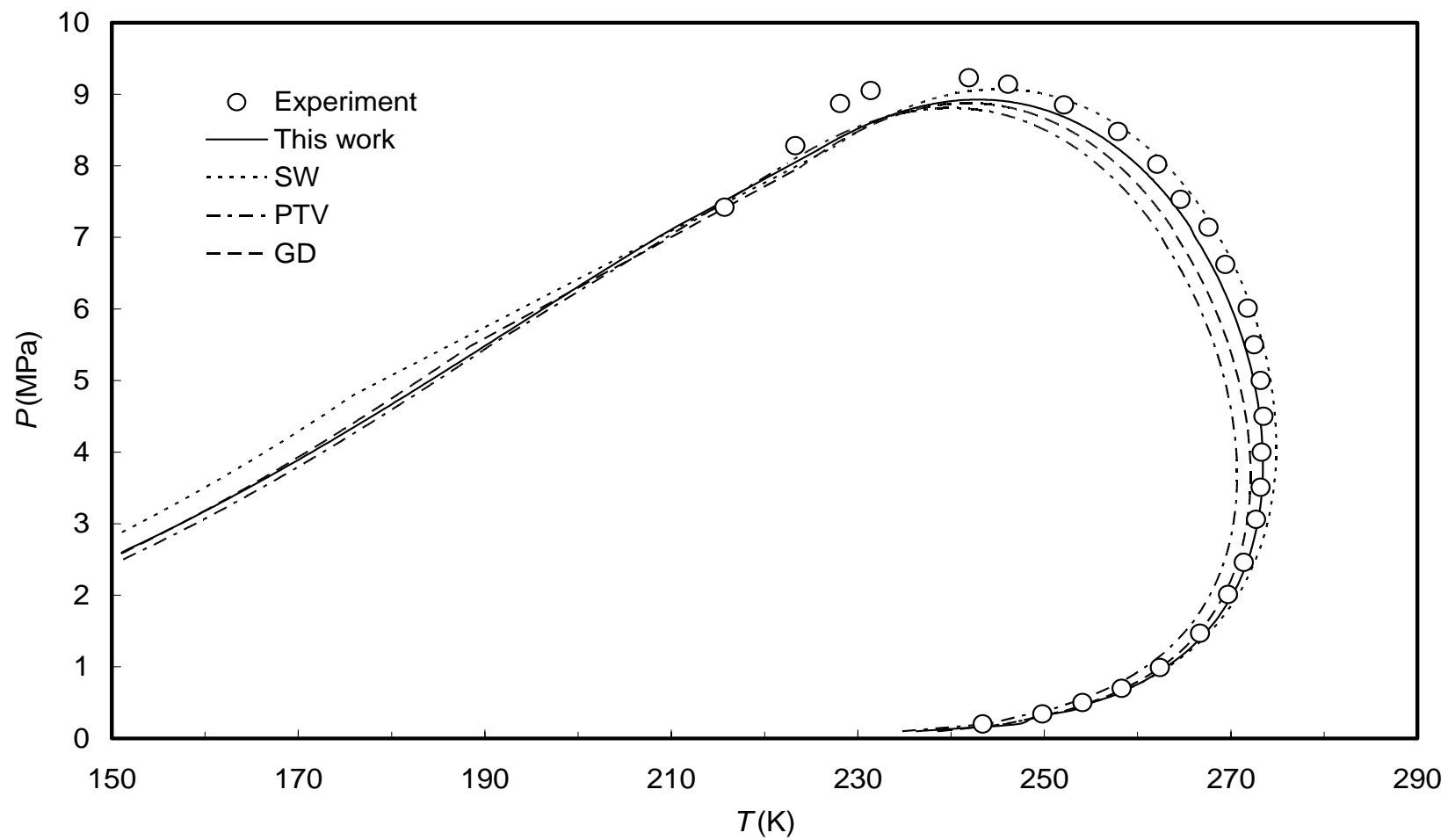


Figure 8.